Contribution from the Institutt for uorganisk kjemi, Norges tekniske høgskole,
Universitetet i Trondheim, N-7034 Trondheim-NTH, Norway

# Complexation and Reduction–Oxidation Equilibria of Titanium Chlorides in Gaseous Aluminum Chloride

MORTEN SØRLIE and HARALD A. ØYE*

*Received December 14, 1977*

$TiCl_2$, $TiCl_3$, and $TiCl_4$ with and without the presence of $Al_2Cl_6$(g) were studied in the gas phase by high-temperature absorption spectroscopy. The following main gaseous species were found: $TiCl_4$, $TiCl_3$, $Ti_2Cl_6$, $TiAlCl_6$, and $TiAl_3Cl_{11}$. Based on ligand field considerations and stoichiometry the following coordinations are suggested: $TiCl_3$ ($C_{3v}$); $Ti_2Cl_6$ and $TiAlCl_6$ (distorted tetrahedral coordination around Ti); $TiAl_3Cl_{11}$ (octahedral coordination around Ti). Thermodynamic data for vaporization and dimerization of $TiCl_3$ and the formation of the gaseous complexes $TiAl_3Cl_{11}$ and $TiAlCl_6$ are given. In the presence of gaseous $Al_2Cl_6$ the stable condensed phases were found to be $TiAl_2Cl_8$(l), $TiCl_2$(s), and $TiCl_3$(s). The presence of $Al_2Cl_6$(g) resulted in a strong enhancement of the apparent vapor pressure of divalent and trivalent titanium; the increase is greatest for titanium in the lowest oxidation state. The gas complexation also resulted in a low-temperature (500–800 K) hot-spot deposition of Ti(s).

## Introduction

The chemistry of titanium chlorides at elevated temperatures is complex due to the interplay of red–ox and vaporization equilibria. The reactions between the pure titanium chlorides of importance in the present study (I–VI) are shown in Table I. These data indicate the stabilities of the different oxidation states of titanium.

The present study is aimed at the thermodynamic and structural characterization of the red–ox and complexation equilibria of titanium chlorides in the presence of the complexing agent aluminum chloride. While the present communication discusses the interactions between titanium chlorides and gaseous aluminum chloride, a subsequent paper[3] will describe the coordination of titanium chlorides in liquid and solid mixtures with aluminum chloride.

$AlCl_3$ is generally found to enhance the volatility of chlorides.[4–6] The volatility and oxidation state will determine the chemical transport of titanium by aluminum chloride, which is of technological importance in connection with two recently proposed aluminum processes, discussed by Grjotheim, Krohn, and Øye,[7] as well as the chlorination of ilmenite for the production of $TiO_2$.[8] Aluminum–titanium chlorides are also important Ziegler–Natta catalysts in the production of polypropylene.[9]

Since titanium chloride compounds absorb light in the visible or near-IR or UV regions, the chosen method of investigation was high-temperature absorption spectroscopy. This is a sensitive method for characterizing the different oxidation states and coordinations. $Ti^{3+}$ and $Ti^{2+}$ also have a simple d-electron configuration ($d^1$ and $d^2$) which enables the use of ligand field theory.

An absorption spectroscopic study not only gives information about the spectra but also can be used for the determination of the vapor pressure of the different components, as demonstrated by Oye and Gruen.[4]

When this method[4] is applied to the present study, a known amount of $TiCl_x$ ($x$ = 2, 3, or 4) is enclosed together with $AlCl_3$ in an optical cell. If the amount of $TiCl_x$ is so small that it evaporates completely (unsaturated vapor), the molar absorptivity of one particular gaseous species, $\epsilon_i$, at wavenumber $i$, is determined according to the Lambert–Beer law

$$\epsilon_i = A_i V/nl \qquad (1)$$

In subsequent experiments it is then possible to determine the pressure of the gaseous molecule from experiments with excess $TiCl_x$ (saturated vapor) by introducing the ideal gas law and rewriting

$$P = A_i R\bar{T}/\epsilon_i l \qquad (2)$$

Table I. Important Equilibria in the Ti–Cl System

| | $\Delta H_{298}°$, kJ | $\Delta S_{298}°$, J/K | ref | eq no. |
|---|---|---|---|---|
| $TiCl_2(s) = TiCl_2(g)$ | 278.4 | 190.9 | 1 | I |
| $3TiCl_2(s) = Ti(s) + 2TiCl_3(g)$ | 468.0 | 402.3 | 1 | II |
| $TiCl_3(s) = TiCl_3(g)$ | 182.5 | 177.7 | 1 | III |
| $Ti_2Cl_6(g) = 2TiCl_3(g)$ | 133.5 | 136.5 | 2 | IV |
| $2TiCl_3(s) = TiCl_2(s) + TiCl_4(g)$ | 164.9 | 162.8 | 1 | V |
| $2TiCl_3(g) = TiCl_2(s) + TiCl_4(g)$ | −200.1 | −191.3 | 1 | VI |

where $A = \log (I_0/I)$ = optical density (absorbance) at wavenumber $i$, $V$ = volume of the cell (L), $n$ = number of moles, $l$ = optical path length (cm), $R$ = gas constant (L atm/(K mol)), $\bar{T}$ = average temperature (K), and $P$ = vapor pressure of light-absorbing species (atm).

If there is more than one light-absorbing species at wavenumber $i$, each species contributes additively to the absorbance.

## Experimental Section

**Apparatus.** Absorption cells for gas spectra were made of cylindrical vitreous silica tubing, inner diameter 24–40 mm, with polished disks of optical quality as windows. All silica tubes and disks ("Spectrosil") were purchased from Thermal Syndicate Ltd., Wallsend, England.

To avoid cracking the cell during the experiments due to tension in the glass, each cell was annealed prior to use. This was done in a furnace by raising the temperature rapidly to 1150 °C and then cooling slowly to less than 200 °C over a 24-h period.

The furnace consisted of a horizontally placed pythagoras tube heated by three Kanthal-wound elements along the tube. Each element was controlled separately by a Eurotherm PID regulator (Eurotherm Ltd., Sussex, England). The two end zones were differentially controlled with respect to the one in the middle. It was thus possible to regulate the temperature gradient to a required profile. The temperature was measured by a calibrated Pt–Pt10%Rh thermocouple close to the middle of the cell while the controlling thermocouples were close to the windings.

To keep the gas cell in a fixed position in the furnace, a rigid cell holder with radiation shields of stainless steel was installed. This arrangement allowed one light beam to pass through the sample cell while the reference beam passed through air outside the furnace.

Figure 1 illustrates an optical cell with a typical temperature profile. The temperatures of the windows of the gas cells were kept 5–20 °C higher than the middle part to avoid transport of the condensed phase into the light path. This figure also shows the transport mechanism of $TiCl_2$(s), which will be discussed later.

The spectrophotometer used in recording the spectra was a CARY Model 17H automatic recording spectrophotometer (Cary Instruments, Monrovia, Calif.), specially suited for high-temperature work.

By means of neutral density screens in the reference beam and manual control of the intensity level which the automatic slit control system is required to maintain, optical densities up to 6 could be measured with the vis-UV detector with good reproducibility. This required in addition the use of a data collection system. The IR detector had, due to a high noise/signal ratio, an upper limit of 3 for the optical density.

0020-1669/78/1317-2473$01.00/0

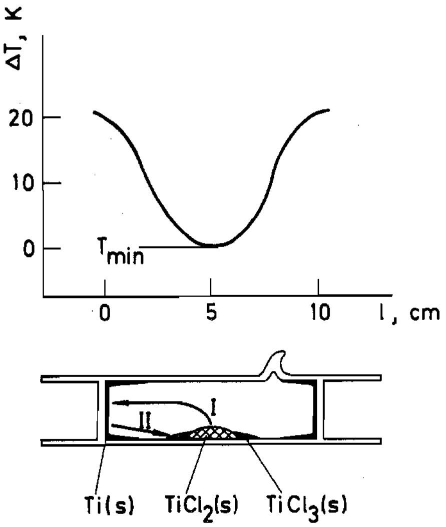

**Figure 1.** Optical cell with typical temperature gradient. Lower figure suggests the decomposition mechanism of the reaction $3TiCl_2(s) = Ti(s) + 2TiCl_3(s)$ in $Al_2Cl_6(g)$: (I) complexation and disproportionation of $TiCl_2(s)$, $TiCl_2(s) + 1.5Al_2Cl_6(g) = TiAl_3Cl_{11}(g)$, $3TiAl_3Cl_{11}(g) = Ti(s) + 3TiAlCl_6(g) + 3.5Al_2Cl_6(g)$; (II) back-transport of $TiCl_3(s)$, $TiAlCl_6(g) = TiCl_3(s) + 0.5Al_2Cl_6(g)$.

Table II. Chemicals

| compd | % purity | manufacturer |
|---|---|---|
| $TiCl_4$ | | made in this laboratory |
| $\alpha$-$TiCl_3$ | 99.9 | K&K Laboratories, Inc. |
| $\alpha$-$TiCl_3$ | | made in this laboratory |
| $TiCl_2$ | | made in this laboratory |
| $Ti(AlCl_4)_2$ | | made in this laboratory |
| Ti | 99.9 | Koch-Light Laboratories Ltd., England |
| $TiO_2$ | $\geqslant$99 | Fluka AG, Switzerland |
| $AlCl_3$ | | made in this laboratory |
| Al | 99.998 | Vigeland Brug, Norway |
| $H_2SO_4$ | p.a. | E. Merck, BRD |
| NaCl | p.a. | E. Merck, BRD |

The data collection system received signals from the spectrophotometer via an interfacing device[10] and transferred the signals to a magnetic tape on an incremental magnetic tape recorder, Model 1600 (Kennedy Co., Altadena, Calif.). With this data collection and recording system, the standard deviation in the optical density for the Cary 17H spectrophotometer has been determined to be $2.2 \times 10^{-3}$ absorption units.

**Chemicals.** The chemicals used in this work are listed in Table II. All chlorides were prepared or purified in the laboratory. Since most of these chlorides are very hygroscopic, they were handled in an inert-atmosphere glovebox ($H_2O$ content < 1 ppm) or under vacuum (pressure $<10^{-5}$ Torr).

Aluminum chloride was produced by reacting Al metal with hydrogen chloride gas at 400 °C. Hydrogen chloride was produced by slowly adding sulfuric acid to solid sodium chloride. The gas was dried by passing it through an acetone/solid carbon dioxide cooling trap before it entered the reaction zone. The aluminum chloride produced was further distilled two to three times to remove the last traces of impurities. This was done in an evacuated and sealed vitreous silica tube. Accurate temperature control was necessary at this step to avoid explosion due to the high vapor pressure of liquid aluminum chloride.

Titanium(IV) chloride was prepared in easily breakable, sealed silica ampules by reacting aluminum chloride with titanium dioxide at 250 °C

$$2Al_2Cl_6(g) + 3TiO_2(s) = 2Al_2O_3(s) + 3TiCl_4(g) \qquad \text{(VII)}$$

Upon cooling of the mixture, $TiCl_4$ was condensed as a colorless liquid in one end of the tube. This end was put into liquid nitrogen and sealed off. The ampule now contained a known amount of $TiCl_4$ which could be stored until used.

Titanium(III) chloride is commercially available in the $\alpha$-$TiCl_3$ modification. This is a flaky powder and contains some adsorbed $TiCl_4$ together with small amounts of oxychlorides. This powder has a tendency to stick to the walls of the silica glass, thus making transfer of small amounts of the salt into the cells difficult.

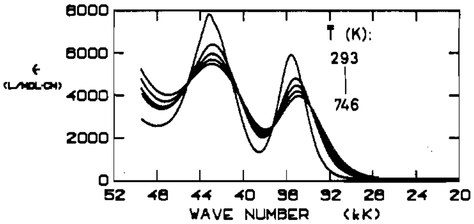

**Figure 2.** Spectra of $TiCl_4(g)$ (experiment 1). The odd shape of the peak with highest absorptivity at $\sim 43 \times 10^3\ cm^{-1}$ is due to smoothing of high noise signals as the limit of instrument detection was reached: $l = 15.0$ cm, $V = 179.9\ cm^3$, $w_{TiCl_4} = 0.002\,20$ g. (1 kK = $10^3\ cm^{-1}$ = 0.1 $\mu m^{-1}$.)

To purify and prepare larger crystals, we made use of the complexing reaction between $TiCl_3$ and $Al_2Cl_6(g)$. This reaction will be discussed in detail latter. $AlCl_3$ and $TiCl_3$ were sealed in an evacuated vitreous silica tube. This tube was heated to about 480 °C in a horizontal furnace with a temperature gradient of a few degrees between the two ends of the tube. Due to the gas complexing reactions and the equilibrium with solid $TiCl_3$, there was a resulting transport of $TiCl_3$ to the colder end of the tube.

The refining procedure gave large, dark violet, shiny crystals. Analysis of the deposit performed by Mikroanalytisches Laboratorium, Bonn, BRD, gave $TiCl_{2.97-3.01}$. It was found that the crystal size was increased by reducing the temperature gradient along the tube.

Titanium(II) chloride prepared according to the methods given by Brauer[11] was not sufficiently pure. The products contained Ti metal or undisproportionated $TiCl_3$ in addition to $TiCl_2$. The method finally adopted was that given by Brynestad et al.,[12] in which Ti metal and liquid aluminum chloride were reacted to form $TiCl_2$–$AlCl_3(l)$ at temperatures between 250 and 300 °C. $Ti(AlCl_4)_2$ can be condensed from the vapor phase of this mixture. The pure crystals or the solidified mixture could be used as such, or $TiCl_2(s)$ could be obtained by disproportionation of the solid at relatively low temperatures (~250 °C) under vacuum

$$Ti(AlCl_4)_2(s) = TiCl_2(s) + Al_2Cl_6(g) \qquad \text{(VIII)}$$

This was done in an evacuated and sealed vitreous silica tube, and $AlCl_3$ was condensed at the colder end of the ampule. $Ti(AlCl_4)_2(s)$ formed bright blue needles, whereas $TiCl_2(s)$ was black, indicating some lack of stoichiometry ($TiCl_{2-x}$).

**Experimental Procedures.** Procedures for charging the cells and recording the spectra have been described previously by Anundskås and Øye.[6]

The spectral data recorded on magnetic tape were processed by computer. Some spectra were taken at both stepwise increasing and decreasing temperatures. Equilibrium conditions were followed by fixing the wavelength and recording the optical density against time.

$\Delta G°$ for the reaction between $Al_2Cl_6(g)$ and silica is negative at the temperatures of this study.[1] In spite of this, only a very slow attack on the cell windows was found at temperatures below 500 °C, probably due to unfavorable kinetics. Light scattering due to this corrosion on the windows gave a continuous rise in the background absorption level during the experiments. The effect was found to increase with temperature. The spectra were corrected for this background absorption.

## Results and Discussion

**Spectra of $TiCl_4$.** The spectrum of $TiCl_4(g)$ is characterized by two absorption bands in the near-UV region with peak positions at 4.28 and ~3.5 $\mu m^{-1}$. The location of the latter band varies from 3.56 $\mu m^{-1}$ at room temperature to 3.49 $\mu m^{-1}$ at 746 K (Figure 2).

The molar absorptivities show marked temperature dependencies, that decrease with increasing temperature. Least-squares polynomial fit for $\epsilon$ vs. $\bar{T}$ gave

$$\epsilon_{3.5} = 5225 - 2.505\bar{T} + (4.306 \times 10^5)/\bar{T} \qquad (3)$$

$$\epsilon_{4.28} = 6440 - 2.301\bar{T} + (5.905 \times 10^5)/\bar{T} \qquad (4)$$

**Table III.** Spectral Characteristics of $TiCl_4(g)$ in the Near-UV Region

| | $3t_2 \rightarrow 2e$ | | $1t_1 \rightarrow 2e$ | | | |
|---|---|---|---|---|---|---|
| $T$, K | $\bar{\nu}$, cm$^{-1}$ × 10$^3$ | $\epsilon$, L/(mol cm) | $\bar{\nu}$, cm$^{-1}$ × 10$^3$ | $\epsilon$, L/(mol cm) | 10$Dq$, cm$^{-1}$ × 10$^3$ | ref |
| 296 | 43.150 | 9000 | 35.650 | 6900 | 7.50 | 13 |
| | 42.8 | 13700$^a$ | 35.4 | 12100$^a$ | 7.4 | 14 |
| | 42.2 | 11800 | 34.8 | 8600 | 7.4 | 15 |
| ~300 | 42.827 | 8100 | 35.600 | 7050 | 7.227 | 16 |
| 293 | 42.8 | 7750 | 35.58 | 5960 | 7.2 | $b$ |
| 516 | 42.86 | 6430 | 35.22 | 4800 | 7.64 | $b$ |
| 586 | 42.80 | 5980 | 35.07 | 4470 | 7.73 | $b$ |
| 667 | 42.83 | 5710 | 34.99 | 4190 | 7.84 | $b$ |
| 746 | 42.83 | 5490 | 34.87 | 3950 | 7.96 | $b$ |

$^a$ Calculated from the published spectrum. $^b$ This work (expt no. 1).

the standard deviations being 21 and 57 L/(mol cm), respectively.

The present study shows reasonable agreement with the investigation of Iverson and Russel[16] and the two bands are considered to be due to the ligand ($p\pi$) → metal (3d) transitions: $1t_1 \rightarrow 2e$ and $1t_1 \rightarrow 3t_2$ (or $2t_2 \rightarrow 2e$).

As the molar absorptivity decreases, a broadening of the half-width of the bands was found, while the oscillator strength remained constant. This is typical for these high-energy transitions and is interpreted as a change in population of the different vibrational levels within an electronic energy state of the $TiCl_4$ molecule.

**$TiCl_3(g)$ and $Ti_2Cl_6(g)$. (a) Spectra and Thermodynamics of Dimerization.** Table IV specifies the conditions of the six experiments in which the temperatures and pressures of $TiCl_3$ and $TiCl_4$ were varied. Experiments 2–4 were carried out with unsaturated $TiCl_3$ vapor in order to obtain molar absorptivities. These experiments were performed with carefully adjusted amounts of $TiCl_3$ and $TiCl_4$ so that $P_{TiCl_4}/(P_{TiCl_3})^2$ was greater than the equilibrium constant $K_{VI}$ in order to avoid formation of $TiCl_2(s)$ in the cells and to have $P_{TiCl_3}$ small enough to ensure complete vaporization. No solid $TiCl_3$ or $TiCl_2$ was observed during the experiments. Experiments 5–7 had excess $TiCl_3(s)$ present. Experiment 7 was the only experiment in which $TiCl_4$ was not added.

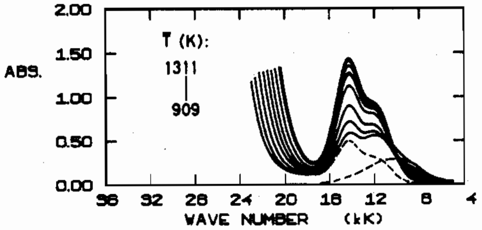

**Figure 3.** Unsaturated vapor spectra of $TiCl_3(g)$ and $Ti_2Cl_6(g)$ (experiment 4). The dotted lines indicate resolved spectra at 909 K.

Neither $TiCl_3$ nor $TiCl_4$ reacted with the vitreous silica cells, and no significant changes in the spectrum were detected after the sample had been kept for more than 24 h at temperatures above 1125 K.

Figure 3 shows the absorption spectra of unsaturated $TiCl_3(g)$ in a $TiCl_4$ atmosphere (experiment 4, Table IV) at temperatures 909–1311 K. At the higher temperatures a

**Table IV.** Spectral Data and Vapor Pressures of $TiCl_3(g)$ and $Ti_2Cl_6(g)$

| | | | | composite spectrum | | $TiCl_3(g)$ | | $Ti_2Cl_6(g)$ | |
|---|---|---|---|---|---|---|---|---|---|
| expt no. | specifications | $T_{min}$, K | $\bar{T}$, K | $A_{1.4}$ | $A_{1.1}$ | $A_{1.43}$ | $P_{TiCl_3}$, atm | $A_{1.05}$ | $P_{Ti_2Cl_6}$, atm |
| 2 | $l = 15.0$ cm | 1067.5 | 1079 | 0.148 | | 0.140 | | | |
| | $V = 168.4$ cm$^3$ | 1087.2 | 1099 | 0.156 | | 0.155 | | | |
| | | 1109.7 | 1121 | 0.171 | | 0.171 | | | |
| | $w_{TiCl_3} = 0.00204$ g | 1141.5 | 1153 | 0.183 | | 0.183 | | | |
| | $w_{TiCl_4} = 0.4344$ g | 1178.5 | 1190 | 0.193 | | 0.193 | | | |
| | | 1216.8 | 1229 | 0.190 | | 0.190 | | | |
| 3 | $l = 15.0$ cm | 1010.0 | 1021 | 0.588 | | 0.550 | | | |
| | $V = 168.4$ cm$^3$ | 1052.2 | 1064 | 0.666 | | 0.640 | | | |
| | | 1094.7 | 1106 | 0.716 | | 0.710 | | | |
| | $w_{TiCl_3} = 0.00924$ g | 1137.3 | 1149 | 0.740 | | 0.740 | | | |
| | $w_{TiCl_4} = 0.4329$ g | 1179.7 | 1192 | 0.748 | | 0.748 | | | |
| | | 1224.1 | 1236 | 0.748 | | 0.748 | | | |
| 4 | $l = 15.0$ cm | 899.1 | 909 | 0.604 | 0.576 | 0.490 | | 0.290 | |
| | $V = 157.8$ cm$^3$ | 953.7 | 964 | 0.737 | 0.618 | 0.680 | | | |
| | | 1008.2 | 1019 | 0.912 | 0.696 | 0.870 | | | |
| | $w_{TiCl_3} = 0.01793$ g | 1062.9 | 1074 | 1.136 | | 1.130 | | | |
| | $w_{TiCl_4} = 0.6765$ g | 1117.1 | 1129 | 1.279 | | 1.279 | | | |
| | | 1116.7 | 1128 | 1.259 | | 1.259 | | | |
| | | 1168.0 | 1180 | 1.357 | | 1.357 | | | |
| | | 1223.9 | 1236 | 1.412 | | 1.412 | | | |
| | | 1277.4 | 1290 | 1.434 | | 1.434 | | | |
| | | 1298.7 | 1311 | 1.439 | | 1.439 | | | |
| 5 | $l = 10.0$ cm | 811.5 | 817 | 0.061 | 0.061 | 0.040 | 0.0019 | 0.040 | 0.0036 |
| | $V = 53.71$ cm$^3$ | 830.8 | 837 | 0.115 | 0.117 | 0.075 | 0.0037 | 0.075 | 0.0070 |
| | | 852.8 | 859 | 0.225 | 0.229 | 0.150 | 0.0076 | 0.150 | 0.0143 |
| | $w_{TiCl_3} = 0.3017$ g | 874.1 | 880 | 0.384 | 0.400 | 0.265 | 0.0137 | 0.275 | 0.0268 |
| | $w_{TiCl_4} = 0.2226$ g | 892.1 | 898 | 0.618 | 0.660 | 0.415 | 0.0218 | 0.450 | 0.0448 |
| | | 905.7 | 911 | 0.898 | 0.987 | 0.640 | 0.0342 | 0.705 | 0.0712 |
| | | 920.9 | 927 | 1.370 | 1.544 | 0.825 | 0.0448 | 1.175 | 0.1208 |
| 6 | $l = 10.0$ cm | 805.0 | 811 | 0.029 | 0.028 | 0.020 | 0.0010 | 0.020 | 0.0018 |
| | $V = 52.55$ cm$^3$ | 857.4 | 863 | 0.180 | 0.182 | 0.120 | 0.0061 | 0.120 | 0.0115 |
| | | 895.5 | 901 | 0.556 | 0.597 | 0.405 | 0.0214 | 0.410 | 0.0410 |
| | $w_{TiCl_3} = 0.2254$ g | 917.5 | 923 | 1.200 | 1.355 | 0.835 | 0.0452 | 0.935 | 0.0957 |
| | $w_{TiCl_4} = 0.4064$ g | 932.9 | 939 | 1.851 | 2.116 | 1.205 | 0.0663 | 1.590 | 0.1644 |
| 7 | $l = 5.0$ cm | 888.5 | 891 | 0.265 | 0.275 | 0.180 | 0.0188 | 0.200 | 0.0395 |
| | $V = 27.32$ cm$^3$ | 910.4 | 912 | 0.475 | 0.503 | 0.335 | 0.0358 | 0.360 | 0.0728 |
| | $w_{TiCl_3} = 0.1258$ g | 932.8 | 935 | 0.961 | 1.037 | 0.565 | 0.0619 | 0.795 | 0.1649 |
| | | 947.9 | 950 | 1.413 | 1.563 | 0.760 | 0.0846 | 1.235 | 0.2602 |
| | | 962.2 | 964 | 2.045 | 2.248 | 0.940 | 0.1062 | 1.850 | 0.3955 |

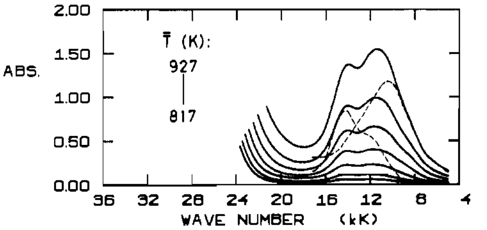

**Figure 4.** Saturated vapor spectra of $TiCl_3(g)$ and $Ti_2Cl_6(g)$ (experiment 5). The dotted lines indicate resolved spectra at 927 K.

double band was observed, with a maximum at 1.43 $\mu m^{-1}$ and a shoulder at ~1.2 $\mu m^{-1}$. At lower temperatures the shoulder at 1.2 $\mu m^{-1}$ was replaced by a peak at about 1.13 $\mu m^{-1}$, accompanied by development of low-energy band shoulders.

The low-energy peak observed for the lowest temperatures of Figure 3 became much more pronounced when the total pressure was increased by having saturated vapor above $TiCl_3(s)$ (Figure 4). Here the peak at 1.13 $\mu m^{-1}$ was observed over the whole temperature range studied and became larger than the peak at around 1.4 $\mu m^{-1}$, which then appeared to be shifted to 1.41 $\mu m^{-1}$. The low-energy shoulders at about 0.6 and 0.9 $\mu m^{-1}$ also become more pronounced.

A comparison between Figure 3 and 4 indicates that there must be more than one light-absorbing species, and the present observations may qualitatively be explained by the existence of dissociation equilibrium IV, which has been reported by Polyachenok et al.[2] and Sibbing and Schäfer.[17]

It is possible to use the present spectroscopic data (experiments 2–7) for the determination of thermodynamic properties for this dissociation of $Ti_2Cl_6(g)$ as well as the vaporization of $TiCl_3(s)$.

This calculation is based first on the observation that the apparent molar absorptivity of the peak around 1.4 $\mu m^{-1}$ was strongly temperature dependent (Table IV), but above 1150–1200 K the temperature dependence became almost negligible, and the intensity ratio for the two transitions at 1.43 and ~1.2 $\mu m^{-1}$ then became constant (Figure 3). The only plausible explanation is that $Ti_2Cl_6(g)$ is completely dissociated above 1150 K (experiments 2–4) and that the peak at 1.43 $\mu m^{-1}$ and the shoulder at ~1.2 $\mu m^{-1}$ are due to temperature-independent transitions of $TiCl_3(g)$. The peak around 1.13 $\mu m^{-1}$ (Figure 4), which decreases with temperature, then is attributed to a transition of $Ti_2Cl_6(g)$ superimposed on a shoulder due to $TiCl_3(g)$.

Secondly, it is assumed that $Ti_2Cl_6(g)$ does not have an absorption maximum at 1.43 $\mu m^{-1}$ where there is a sharp absorption peak due to $TiCl_3(g)$.

It is then possible to decompose the composite spectra of $TiCl_3(g)$ and $Ti_2Cl_6(g)$ as shown in Figures 3 and 4. The spectrum at 1311 K (Figure 3) is taken as the spectrum of $TiCl_3(g)$ at all temperatures and is subtracted from composite spectra, requiring that the difference spectra of $Ti_2Cl_6(g)$ do not exhibit a maximum or minimum around 1.43 $\mu m^{-1}$. This is done by a trial and error procedure using different scaling factors for the $TiCl_3(g)$ spectrum. This procedure worked well for all spectra except when the amount of $Ti_2Cl_6(g)$ was very small. Table IV gives the net absorptivities due to $TiCl_3(g)$ (experiments 2–4) and for both $TiCl_3(g)$ and $Ti_2Cl_6(g)$ (experiments 5–7).

It was found practical to perform the thermodynamic calculations differently in experiments with unsaturated (experiments 2–4) and saturated vapor (experiments 5–7).

For the experiments with unsaturated vapor the total amount of trivalent titanium in the gas phase was known, and the equilibrium constant of reaction IV could be determined from the decrease in $TiCl_3(g)$ absorption at 1.43 $\mu m^{-1}$ combined with a mass balance and the Lambert–Beer law

$$A_{1.43} = \frac{\epsilon_{1.43} l}{4RT}\{(K_{IV}^2 + 8K_{IV}P_{TiCl_3}{}^\circ)^{1/2} - K_{IV}\} \qquad (5)$$

where $A_{1.43}$ is the *net* optical density of $TiCl_3(g)$ and $\epsilon_{1.43}$ is the molar absorptivity of $TiCl_3(g)$ at the same wavenumber. $P_{TiCl_3}{}^\circ$ is the vapor pressure calculated from the ideal gas law without correcting for dimerization.

$\Delta S_{IV}{}^\circ$ and $\Delta H_{IV}{}^\circ$ were assumed to be temperature independent in the range studied

$$RT \ln K_{IV} = -\Delta H_{IV}{}^\circ + T\Delta S_{IV}{}^\circ \qquad (6)$$

By use of a nonlinear regression analysis[18] on the data for experiments 2–4, the parameters $\epsilon_{1.43}$, $\Delta H_{IV}{}^\circ$, and $\Delta S_{IV}{}^\circ$ were found. With an overall standard deviation of 7% in $A_{1.43}$ we obtain $\epsilon_{1.43} = 140 \pm 4$ L/(mol cm), $\Delta H_{IV}{}^\circ = 137 \pm 10$ kJ, and $\Delta S_{IV}{}^\circ = 116 \pm 10$ J/K. These data give the following expression of $K_{IV}$

$$K_{IV} = \exp\left(6.042 - \frac{7143}{T}\right) \qquad (7)$$

For the experiments with $TiCl_3(s)$ present (experiments 5–7), the gas phase is saturated, and the pressures of $TiCl_3(g)$ and $Ti_2Cl_6(g)$ can be calculated from eq 2 when the molar absorptivities of the absorbing species are known. The previous experiments 2–4 already have established the molar absorptivity of $TiCl_3$ as $\epsilon_{1.43} = 140$ L/(mol cm). The corresponding values of $P_{TiCl_3}$ according to equilibrium III are again found from the *net* absorption of $TiCl_3$, $A_{1.43}$, listed in Table IV.

Neglecting $\Delta C_p$, we have

$$\frac{d \ln P_{TiCl_3}}{d(1/T)} = -\frac{\Delta H_{III}{}^\circ}{R} \qquad (8)$$

and we find $\Delta H_{III}{}^\circ = 181 \pm 20$ kJ and $\Delta S_{III}{}^\circ = 170 \pm 19$ J/K, in reasonably good agreement with JANAF data (Table I). Values of $P_{TiCl_3}$ below 850 K have been omitted in this calculation due to low absorption of $Ti_2Cl_6(g)$ and uncertain resolution.

Due to the relatively low concentration of $Ti_2Cl_6(g)$ in experiments 2–4, the molar absorptivity of $Ti_2Cl_6$, $\epsilon_{1.05}$, could be obtained with less accuracy. By use of values for $T < 1000$ K it was concluded that $\epsilon_{1.05} = 74$ L/(mol cm). For these temperatures the spectrum of $Ti_2Cl_6(g)$ had the same appearance as those found in experiments 5–7, but at higher temperatures, however, the band starts to change shape. Above 1020 K it is split into two separate bands, one at 1.12 $\mu m^{-1}$ and one at 0.9 $\mu m^{-1}$, the latter having a shoulder at 0.6 $\mu m^{-1}$. As a very rough estimate we chose to use a constant $\epsilon_{1.05} = 74$ L/(mol cm) as the net molar absorptivity of $Ti_2Cl_6(g)$.

The corresponding pressures of $Ti_2Cl_6$ calculated from eq 2 are given in Table IV, and the thermodynamic data for the reaction

$$2TiCl_3(s) = Ti_2Cl_6(g) \qquad (IX)$$

were found to be $\Delta H_{IX}{}^\circ = 218 \pm 25$ kJ and $\Delta S_{IX}{}^\circ = 219 \pm 25$ J/K, in close agreement with the values given by Polyachenok et al.,[2] $\Delta H_{IX}{}^\circ = 229$ kJ and $\Delta S_{IX}{}^\circ = 226$ J/K, and by Sibbing and Schäfer,[17] $\Delta H_{IX}{}^\circ = 217$ kJ and $\Delta S_{IX}{}^\circ = 213$ J/K. Furthermore we have

$$2(\text{reaction III}) - \text{reaction X} = \text{reaction IV} \qquad (9)$$

Experiments 5–7 yield the following values for reaction IV: $\Delta H_{IV}{}^{\circ\prime} = 143 \pm 29$ kJ, $\Delta S_{IV}{}^{\circ\prime} = 122 \pm 24$ J/K.

We consider the agreement with the previously calculated values of 137 kJ and 116 J/K to be very satisfactory, and a small temperature dependence in $\epsilon_{1.05}$ might render the correlation even better. Figure 5 summarizes the calculation of $K_{IV}$. Data from experiments 2–4 are given as a line and those from experiments 5–7 as points. Only Polyachenok et

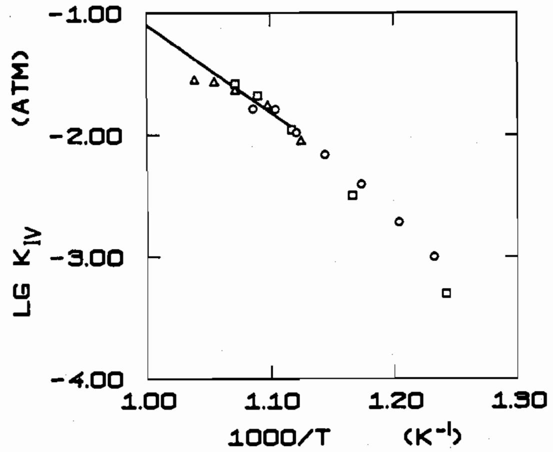

**Figure 5.** Equilibrium constant for the dissociation reaction $Ti_2Cl_6(g) = 2TiCl_3(g)$: —, calculated from experiments 2–4; ○, experiment 5; □, experiment 6; △, experiment 7.

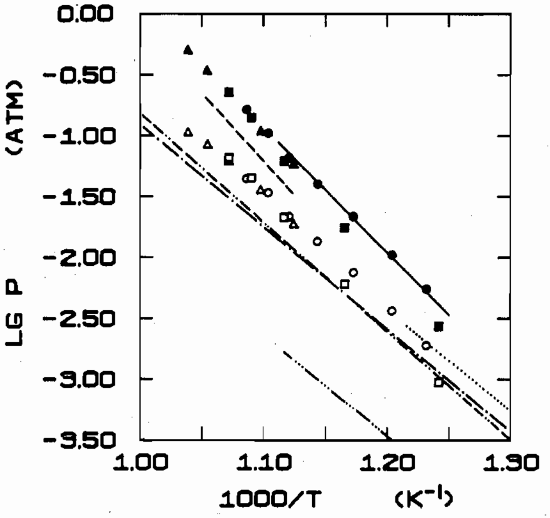

**Figure 6.** Sublimation pressure of trivalent titanium chloride: open symbols, partial pressure of monomer, $P_{TiCl_3}$; filled symbols, total vapor pressure, $P_{TiCl_3+Ti_2Cl_6}$; ○,●, experiment 5; □,■, experiment 6; △,▲, experiment 7; --···--, JANAF, $P_{TiCl_3}$; —, Polyachenok et al.,[2] $P_{TiCl_3+Ti_2Cl_6}$; ---, Sibbing and Schäfer,[17] $P_{TiCl_3+Ti_2Cl_6}$; -···, Gross,[19] $P_{TiCl_3}$, no dimerization reported; -····-, Altman et al.,[20] $P_{TiCl_3}$ (extrapolated), no dimerization reported; ···, Sanderson and MacWood,[21,22] $P_{TiCl_3}$, no dimerization reported.

al.[2] and Sibbing and Schäfer[17] have reported the formation of titanium trichloride dimer in the vapor phase. Our data agree well with those of Sibbing and Schäfer whereas Polyachenok et al. have $TiCl_3(g)$ as the dominant species in the temperature range studied. This is contrary to the present results, from which the dimer is found to have a higher vapor pressure than the monomer in equilibrium with $TiCl_3(s)$. We expect the dimer to dominate in spite of the fact that the assumption of a temperature-independent molar absorptivity may not be strictly valid. According to the structural interpretation of the spectra, to be discussed later, a temperature dependence, analogous to what we find for the $Ti^{3+}$–Al–Cl(g) complex, would be expected. Hence, the molar absorptivity values are expected to increase somewhat with increasing temperature. The vapor pressure of $Ti_2Cl_6(g)$ and the total pressure then will be a little higher at temperatures below 909 K and a little lower at temperatures above 909 K. This would confirm the dimer ⇄ monomer equilibrium to Brewer's rule[23] which predicts, from simple thermodynamic reasons, that the minor species becomes more prevalent at higher temperatures provided a condensed phase is present.

In Figure 6 are plotted the total pressure ($P_{Ti_2Cl_6} + P_{TiCl_3}$) and $P_{TiCl_3}$ above $TiCl_3(s)$ from experiments 5–7. The data are compared with values from the literature.

The total sublimation pressure of titanium trichloride can be expressed by the empirical correlation

$$P_{TiCl_3+Ti_2Cl_6} = \exp\left(10.95 - \frac{10830}{T}\right) \qquad (10)$$

and corresponds well with the total pressure given by Polyachenok et al.[2] Their tensimetric method is expected to give the total pressure with good accuracy.

**(b) Coordination.** The electronic structure of $TiCl_3$ with one unpaired electron will probably lead to $C_{3v}$ symmetry. In the JANAF Tables,[1] $C_{3v}$ symmetry has been listed as the most probable, and the bond angles have been estimated on this assumption. The two bands are then probably due to the transition $^2A \rightarrow {}^2E$ with a Jahn–Teller instability of the exited $^2E$ state. The high molar absorptivity values indicate d–p mixing of the orbitals.

In view of the differences in the spectra of $TiCl_3(g)$ and $Ti_2Cl_6(g)$, the ligand field symmetry of $Ti_2Cl_6$ must be different from that observed for the monomer.

A reasonable structure for $Ti_2Cl_6$ is to assume that it is similar to $Fe_2Cl_6$ and $Al_2Cl_6$ with a distorted tetrahedral symmetry around $Ti^{3+}$. Hence, the molecule can be visualized as two strongly deformed tetrahedra sharing one edge. The observed bands do not contradict such an interpretation. By the symmetry descent $T_d \rightarrow D_{2d} \rightarrow C_{2v}$, the degeneracy of the terms will be lifted completely. We observe three transitions at 1.05, 0.9, and 0.6 $\mu m^{-1}$. With $A_1$ as the ground state we probably observed $A_1 \rightarrow B_2'$, $A_1 \rightarrow B_2''$, and $A_1 \rightarrow A_2$.

The same model of local symmetry around $Ti^{3+}$ in $Ti^{3+}$–Al–Cl gas complexes, which are discussed later, was adopted.

**$TiCl_4(g)$ with $Al_2Cl_6(g)$.** Contrary to what was found for mixtures of $TiCl_4$ with $AlCl_3(s)$ and $Al_2Cl_6(l)$,[3] mixtures of $TiCl_4(g)$ and $Al_2Cl_6(g)$ did not show any shift in the high-energy absorption edge toward lower energies compared with pure $TiCl_4(g)$ at temperatures ~475–800 K.

Possible gas complexation also could be investigated by more indirect means. By a study of the reaction

$$TiCl_3(s) + nAl_2Cl_6(g) = TiAl_{2n}Cl_{6n+3}(g) \qquad (X)$$

with and without $TiCl_4$ added, a reaction between $TiCl_4$ and $Al_2Cl_6$ would consume $Al_2Cl_6(g)$ and thus reduce the amount of $TiAl_{2n}Cl_{6n+3}(g)$ formed. Data from this study are given in the next chapter in connection with the $TiCl_3$ gas complexation. It was found that experiment 11, in which no $TiCl_4(g)$ was added, did not give a different equilibrium constant for reaction X than experiments 12–14, when $TiCl_4(g)$ was added (Table V and Figure 9). Therefore it is concluded that gas complexation between $TiCl_4$ and $Al_2Cl_6$ is of no importance.

**$TiCl_3(g)$ with $Al_2Cl_6(g)$. (a) Spectra and Thermodynamics of Gas Complexation.** Vaporization of $TiCl_3$ with $Al_2Cl_6(g)$ was studied at lower temperatures than those used in the experiments without $Al_2Cl_6$. At these lower temperatures, the contribution to the spectra of $TiCl_3(g)$ and $Ti_2Cl_6(g)$ was found to be negligible. Table V specifies the different experiments. Experiments 8–10 were carried out with unsaturated $TiCl_3$ vapor in order to obtain the molar absorptivity of the gas complex, and experiments 11–14 had excess $TiCl_3(s)$ in order to determine the complexation equilibria. Varying amounts of $TiCl_4$ were added in order to counteract the disproportionation of $TiCl_3$.

The presence of $Al_2Cl_6(g)$ together with $TiCl_3$ in the cell gave a totally different spectrum (Figure 7) from that of pure $TiCl_3(g)$ (Figures 3 and 4), showing that a complexing reaction occurs in the gas phase. A composite band was found with the main peak at 1.09 $\mu m^{-1}$ and shoulders at 0.6, 0.9, and 1.4 $\mu m^{-1}$. At the lowest recorded temperatures, the shoulders at

**Table V.** Spectral Data and Vapor Pressures of $Ti^{3+}$–Al–Cl Complexes

| expt no. | specifications | $T_{min}$, K | $\bar{T}$, K | $A_{10.9}$ | $\epsilon_{1.09}$, L/(mol cm) | $P_{Al_2Cl_6}$,[a] atm | $P_{Ti^{3+}-Al-Cl}$, atm |
|---|---|---|---|---|---|---|---|
| 8 | $l = 10.0$ cm | 850.5 | 854 | 0.413 | 18.39 | | |
| | $V = 46.53$ cm$^3$ | 795.9 | 800 | 0.291 | 12.98 | | |
| | $w_{TiCl_3} = 0.0161$ g | 742.5 | 746 | 0.195 | 8.69 | | |
| | $w_{AlCl_3} = 1.240$ g | 688.4 | 692 | 0.116 | 5.17 | | |
| | $w_{TiCl_4} = 0.0755$ g | 690.6 | 694 | 0.118 | 5.27 | | |
| | | 745.1 | 749 | 0.197 | 8.78 | | |
| | | 855.0 | 859 | 0.425 | 18.94 | | |
| 9 | $l = 10.0$ cm | 837.8 | 849 | 0.683 | 18.21 | | |
| | $V = 52.40$ cm$^3$ | 817.3 | 828 | 0.582 | 15.53 | | |
| | $w_{TiCl_3} = 0.0303$ g | 895.9 | 807 | 0.505 | 13.48 | | |
| | $w_{AlCl_3} = 1.0174$ g | 774.6 | 785 | 0.429 | 11.45 | | |
| | | 744.3 | 755 | 0.332 | 8.87 | | |
| 10 | $l = 10.0$ cm | 832.5 | 839 | 0.436 | 17.71 | | |
| | $V = 52.44$ cm$^3$ | 810.8 | 818 | 0.382 | 15.51 | | |
| | $w_{TiCl_3} = 0.0199$ g | 789.3 | 796 | 0.329 | 13.39 | | |
| | $w_{AlCl_3} = 0.8269$ g | 767.0 | 774 | 0.278 | 11.31 | | |
| | $w_{TiCl_4} = 0.1417$ g | 745.9 | 753 | 0.232 | 9.44 | | |
| | | 724.4 | 731 | 0.192 | 7.79 | | |
| | | 702.3 | 709 | 0.157 | 6.40 | | |
| | | 681.4 | 688 | 0.122 | 4.94 | | |
| 11 | $l = 10.0$ cm | 816.2 | 826 | 2.245 | | 3.942 | 0.965 |
| | $V = 50.77$ cm$^3$ | 792.8 | 803 | 1.506 | | 4.043 | 0.733 |
| | $w_{TiCl_3} = 0.7108$ g | 771.4 | 782 | 0.992 | | 4.105 | 0.547 |
| | $w_{AlCl_3} = 1.0003$ g | 739.8 | 750 | 0.519 | | 4.127 | 0.352 |
| | | 705.6 | 716 | 0.251 | | 4.074 | 0.221 |
| 12 | $l = 10.0$ cm | 831.4 | 842 | 2.487 | | 2.431 | 0.988 |
| | $V = 51.38$ cm$^3$ | 810.6 | 821 | 1.669 | | 2.569 | 0.737 |
| | $w_{TiCl_3} = 0.7313$ g | 789.5 | 800 | 1.102 | | 2.665 | 0.546 |
| | $w_{AlCl_3} = 0.6877$ g | 765.9 | 776 | 0.714 | | 2.719 | 0.408 |
| | $w_{TiCl_4} = 0.1490$ g | 733.9 | 744 | 0.368 | | 2.750 | 0.260 |
| | | 701.5 | 712 | 0.181 | | 2.730 | 0.165 |
| 13 | $l = 10.0$ cm | 832.9 | 840 | 1.442 | | 0.963 | 0.579 |
| | $V = 51.70$ cm$^3$ | 813.0 | 820 | 0.988 | | 1.049 | 0.439 |
| | $w_{TiCl_3} = 0.2570$ g | 790.2 | 797 | 0.654 | | 1.118 | 0.329 |
| | $w_{AlCl_3} = 0.3191$ g | 767.3 | 774 | 0.424 | | 1.168 | 0.245 |
| | $w_{TiCl_4} = 0.1414$ g | 734.9 | 742 | 0.232 | | 1.202 | 0.167 |
| | | 702.0 | 708 | 0.116 | | 1.212 | 0.109 |
| 14 | $l = 10.0$ cm | 837.1 | 847 | 0.952 | | 0.301 | 0.369 |
| | $V = 52.86$ cm$^3$ | 815.5 | 826 | 0.664 | | 0.353 | 0.286 |
| | $w_{TiCl_3} = 0.4228$ g | 793.2 | 804 | 0.450 | | 0.399 | 0.219 |
| | $w_{AlCl_3} = 0.1393$ g | 771.4 | 782 | 0.304 | | 0.434 | 0.168 |
| | $w_{TiCl_4} = 0.1426$ g | 735.7 | 746 | 0.147 | | 0.476 | 0.103 |

[a] $P_{Al_2Cl_6}$, partial pressure of $Al_2Cl_6$, corrected for dissociation and complexation.

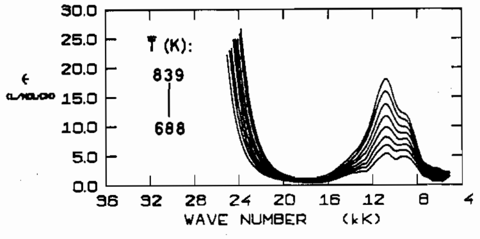

**Figure 7.** Spectra of $Ti^{3+}$–Al–Cl(g) (experiment 10).

0.9 and 1.4 μm$^{-1}$ were seen as definite peaks.

The molar absorptivity of the main peak at 1.09 μm$^{-1}$ was found to be highly temperature dependent, increasing by a factor of ~4 from 690 to 860 K. The results from experiments 8–10 are plotted in Figure 8, in which molar absorptivity vs. average temperature over the cell is shown. A least-squares polynomial fit yields for the main peak at 1.09 μm$^{-1}$

$$\epsilon_{1.09} = 43.90 - 0.1684\bar{T} + (1.626 \times 10^{-4})\bar{T}^2 \quad (11)$$

with a standard deviation of 0.34 L/(mol cm).

The $TiAl_{2n}Cl_{6n+3}$ gas complexes, which for simplicity will be denoted as $Ti^{3+}$–Al–Cl, were stable in the temperature range studied. However, a small degree of disproportionation of $TiCl_3$ was observed. In the experiments where no $TiCl_4$ was added (experiments 9 and 11), small amounts of it could be detected after the run. This could be seen from a slight yellow discoloration of the $AlCl_3$ crystals. Both $AlCl_3$(s) and $TiCl_4$(l) are colorless at room temperature, but, upon mixing, the solid

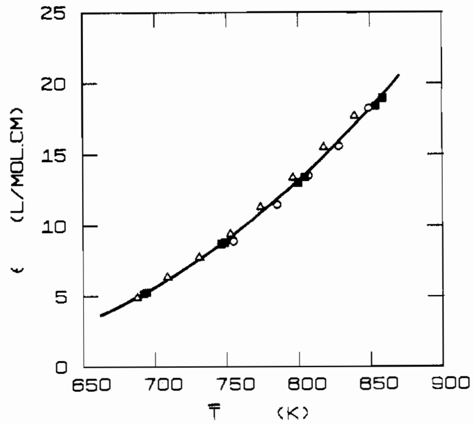

**Figure 8.** Molar absorptivity of $Ti^{3+}$–Al–Cl(g) at 1.09 μm$^{-1}$: ■, experiment 8; ○, experiment 9; △, experiment 10.

**Table VI.** Calculation of Stoichiometric Constant *n* in Equation X (with $TiCl_3$), Choosing Experiment 12 as the Common Reference[a]

| expt | 833 K | 800 K | 769 K | 741 K | 714 K |
|---|---|---|---|---|---|
| 12-11 | 0.54 | 0.56 | 0.56 | 0.57 | 0.57 |
| 12-13 | 0.62 | 0.62 | 0.61 | 0.58 | 0.54 |
| 12-14 | 0.51 | 0.53 | 0.53 | 0.51 | 0.48 |

[a] $\bar{n} = 0.56 \pm 0.04$.

$AlCl_3$-rich phase becomes deep yellow due to interaction with $TiCl_4$.[3]

Furthermore, $TiCl_4(g)$ in the cells could be detected by the fog-forming oxidation to $TiO_2$ upon opening the cells in air.

Disproportionation of $TiCl_3$ gives small amounts of $TiCl_2$, which would be expected to react with $Al_2Cl_6(g)$ to form a $Ti^{2+}$–Al–Cl complex. This was found to occur to some extent, and the shoulder at $\sim 1.4\ \mu m^{-1}$ (Figure 7) is attributed to this reaction (see next section). However, all experiments with $TiCl_3(s)$ in equilibrium with $Al_2Cl_6(g)$ (experiments 11–14) were carried out at temperatures where $K_V$ ($=P_{TiCl_4}$) $\ll 1$ (i.e., disproportionation reaction V is strongly shifted to the left-hand side).

In the experiments for determining the molar absorptivity of the complex, $TiCl_4$ was added to two cells (experiments 8 and 10) but not to the third (experiment 9). The calculated molar absorptivity for experiment 9 did not show any significant deviation from the values of the other two, which shows that errors due to disproportionation of $TiCl_3$ are negligible.

The molar absorptivity values do not seem to be significantly dependent on either the aluminum chloride pressure or the amount of $TiCl_3$ added to the cell in the temperature range studied. It is therefore to be concluded that mainly mononuclear titanium complex molecules exist in the vapor phase, and if more than one species are present they will have approximately the same molar absorptivity.[4]

The stoichiometry and thermodynamics of this complexation reaction were determined from experiments 11–14.

The apparent pressure of aluminum chloride, $P_{Al_2Cl_6}{}^{\circ}$, was varied by a factor of 7.5. A detailed procedure for obtaining thermodynamic data is given by Øye and Gruen.[4]

Using experiment 12 as the common reference, we find the stoichiometric constant, *n*, to be 0.56 ± 0.04 (Table VI), thus giving a hypothetical complexation reaction

$$TiCl_3(s) + 0.56Al_2Cl_6(g) = TiAl_{1.12}Cl_{6.36}(g) \qquad (XI)$$

which is consistent with the presence of two complex species, for instance $TiAlCl_6$ and $TiAl_2Cl_9$, in equilibrium with the solid. Figure 9 presents $\log K_{XI}$ vs. $1/T$. Fitting $\log K_{XI}$ to a function of the type

$$\log K = A + B/T + C/T^2 \qquad (12)$$

we obtain

$$\log K_{XI} = 11.32 - (14.68 \times 10^3)/T + (4.225 \times 10^6)/T^2 \qquad (13)$$

with a standard deviation corresponding to 4.7% over the temperature range studied. Since $n = 0.56$, the main complex species is $TiAlCl_6(g)$. However, this cannot be the only type of complex molecule present in the gas. This may be seen from Figure 9, in which there is no linear relationship between $\log K_{XI}$ and $1/T$, and also from the trend of the experimental vapor pressures which are plotted in Figure 10. We observe a positive curvature, i.e., $d^2 \log P/d(1/T)^2 > 0$.

Using a computer program developed by Hertzberg[18] the data could be fitted to models with different types of complex species present according to equations of the type

$$P_{Ti^{3+}\text{-}Al\text{-}Cl} = \sum P_{Al_2Cl_6}{}^{n_j} \exp(A_j + B_j/T) \qquad (14)$$

where $n_j$ is the stoichiometric constant for the *j*th complex species.

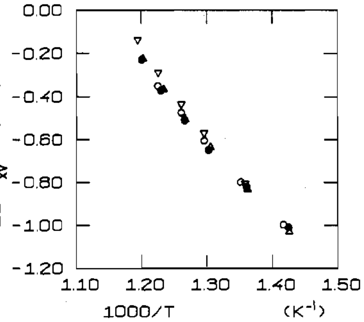

**Figure 9.** Equilibrium constant for the hypothetical reaction $TiCl_3(s) + 0.56Al_2Cl_6(g) = TiAl_{1.12}Cl_{6.36}(g)$: ○, experiment 11; △, experiment 12; ●, experiment 13, ▽, experiment 14.

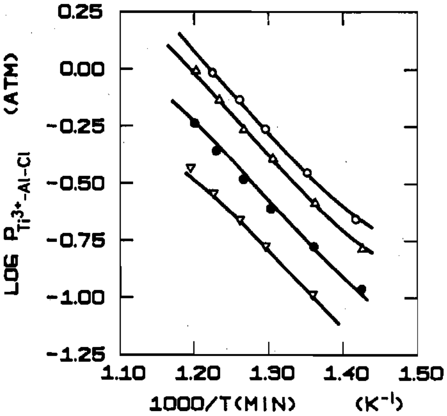

**Figure 10.** Experimental vapor pressure of $Ti^{3+}$–Al–Cl(g) complexes in equilibrium with $TiCl_3(s)$ and $Al_2Cl_6(g)$: ○, experiment 11; △, experiment 12; ●, experiment 13; ▽, experiment 14; —, eq 15.

We have tested different models with two different species present simultaneously. The data are not considered sufficiently accurate for three species to be taken into consideration.

The best description of our experimental data gives a two-species model with $n_j = 0.5$ and 1.0. The equilibria then can be written as

$$TiCl_3(s) + {}^1/_2Al_2Cl_6(g) = TiAlCl_6(g) \qquad (XII)$$

and

$$TiCl_3(s) + Al_2Cl_6(g) = TiAl_2Cl_9(g) \qquad (XIII)$$

with the former dominating over the entire temperature range. The corresponding pressure equation is

$$P_{Ti^{3+}\text{-}Al\text{-}Cl} = \exp\left(4.633 - \frac{4036}{T}\right)P_{Al_2Cl_6}{}^{1/2} + \exp\left(-4.979 + \frac{2240}{T}\right)P_{Al_2Cl_6} \qquad (15)$$

The overall standard deviation in $P_{Ti^{3+}\text{-}Al\text{-}Cl}$ was 4.3%. Curves corresponding to this model have been drawn in Figure 10. The experimental values are probably inaccurate at the lowest temperatures. This can be seen from the second part of eq 15 where the calculated numbers have opposite signs from what is expected thermodynamically. The standard deviations in these parameters are of the same magnitude as the computed numbers, meaning that they are coupled in such a way that their individual numerical values are of little thermodynamic significance. This also implies that eq 15 should not be used at temperatures lower than those measured.

The parameters in the first part of eq 15 describe, however, nearly the whole set of experimental data and are not much affected by changes in the second term. Thermodynamic

**Table VII.** Spectral Characteristics of $Ti^{3+}$

| system | $T$, K | $\bar{\nu}$, $cm^{-1}$ × $10^3$ | $\epsilon$, L/(mol cm) | $\bar{\nu}$, $cm^{-1}$ × $10^3$ | $\epsilon$, L/(mol cm) | coord | ref |
|---|---|---|---|---|---|---|---|
| $\alpha$-$TiCl_3$(s) | 295 | 14.3 | ~$10^a$ | 18.9 | ~100 | $O_h$ | 24 |
| $TiCl_3$ in $CsGaCl_4$(l) | 873 | 6.2 | ~25 | 12.3 | ~18 | $O_h \rightleftarrows T_d$ | 25 |
| $TiCl_3$ in $CsGaCl_4$(l) | 1173 | 8.5 | ~50 | | | $O_h \rightleftarrows T_d$ | 25 |
| $TiCl_3$ in LiCl-KCl(l) eutectic | 673 | 10.6 | ~3 | 13.2 | ~4 | $O_h \rightleftarrows T_d$ | 25 |
| $TiCl_3$ in LiCl-KCl(l) eutectic | 1273 | 6.8 | ~7 | 12.3 | ~11 | $O_h \rightleftarrows T_d$ | 25 |
| $TiCl_3$(g) | 900-1300 | 14.3 | 140 | | | $C_{3v}$ | this work |
| $Ti_2Cl_6$(g) | 909 | 10.5 | 74 | | | $C_{2v}$ | this work |
| $TiCl_3$ in $Al_2Cl_6$(g) | 692 | 10.9 | 5.2 | | | $C_{2v}$ | this work |
| $TiCl_3$ in $Al_2Cl_6$(g) | 859 | 10.9 | 18.9 | | | $C_{2v}$ | this work |

[a] Calculated from the published spectrum.

values for formation of the main gaseous species, $TiAlCl_6$, are thus $\Delta H_{XII}° = 77.3 \pm 2.6$ kJ and $\Delta S_{XII}° = 88.7 \pm 3.2$ J/K.

The calculation of $P_{Al_2Cl_6}$ is based on the ideal gas law using the weighed-in amount of $AlCl_3$ corrected for dissociation and complexing reactions. Thermodynamic values for the dissociation of $Al_2Cl_6$(g)

$$Al_2Cl_6(g) = 2AlCl_3(g) \qquad (XIV)$$

were taken from JANAF.[1]

A comparison of the vapor pressure of $TiAlCl_6$ in 1 atm of $Al_2Cl_6$ with that of $TiCl_3$ above $TiCl_3$(s)[1] at 800 K shows an increase in volatility by a factor of 500. This is a smaller increase than has been observed for transition-metal chlorides with a lower vapor pressure for the pure component.[6]

Combination of reactions IX and XII yields

$$^1/_2Ti_2Cl_6(g) + {}^1/_2Al_2Cl_6(g) = TiAlCl_6(g) \qquad (XV)$$

with $\Delta H_{XV}° = -32$ kJ and $\Delta S_{XV}° = -21$ J/K. It is somewhat surprising that the entropy is not closer to zero. Part of the discrepancy may be due to standard deviation in the determination of $\Delta S°$ for reaction IX and XII. However, $\Delta S_{IX}°$ is in excellent agreement with Polyachenok et al.[2] and Sibbing and Schäfer[17] while the data for reaction XII could be fitted with as low as a standard deviation of 4.3%.

**(b) Coordination.** The stoichiometry of the complex molecule, $TiAlCl_6$(g), excludes octahedral or near-octahedral symmetry of the ligands around the central atom. A molecule with two tetrahedra sharing one edge with $Ti^{3+}$ in a tetrahedral field also must be excluded due to the low molar absorptivity values and their high-temperature dependence, which is contrary to what is expected in $T_d$ symmetry.

Following the same reasoning as with $Ti_2Cl_6$(g), and noting the resemblance of the two specra, we consider the local symmetry to be $C_{2v}$. The $TiAlCl_6$(g) molecule probably will consist of a distorted chlorine tetrahedron around the aluminum atom sharing one edge with a heavily distorted chlorine tetrahedron around the titanium atom. The molar absorptivity of $TiAlCl_6$(g) is, however, only about one-third of that of $Ti_2Cl_6$(g). This need not be at variance with a $C_{2v}$ symmetry because this coordination spans geometries from nearly square planar to nearly tetrahedral, with a resulting difference in orbital interaction. A more pronounced energy splitting of $TiAlCl_6$(g) relative to $Ti_2Cl_6$(g) is also noted. The splitting of the free ion term in the $C_{2v}$ field gives an $A_1$ term as the ground state. The three observed peaks (shoulders) at 1.09, 0.9, and 0.6 $\mu m^{-1}$ then can be interpreted in the same way as for $Ti_2Cl_6$, $A_1 \rightarrow B_2'$, $A_1 \rightarrow B_2''$ and $A_1 \rightarrow A_2$.

We are, however, not able to offer an explanation of the unusually large temperature variation of the molar absorptivity (Figure 8).

Spectral characteristics of $Ti^{3+}$ in different solvents are listed in Table VII.

**$TiCl_2$(g) with $Al_2Cl_6$(g). (a) Spectra and Thermodynamics of Gas Complexation.** Studies of the gaseous complexation between $TiCl_2$ and $Al_2Cl_6$ proved to be difficult experimentally. Even with the utmost care in avoiding small impurities of water, oxygen, or titanium in other oxidation states, a disproportionation according to reaction II was observed.

With time a film of Ti metal was deposited on the walls inside the cell. This is accompanied by a rising background absorption level which rendered the cell opaque to light within a few hours.

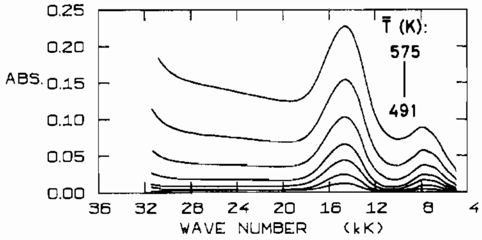

**Figure 11.** Spectra of $Ti^{2+}$–Al–Cl(g) (experiment 15).

In an attempt to obtain the spectrum of gaseous species of $Ti^{2+}$ at high temperatures, a mixture of $Ti(AlCl_4)_2$ and $AlCl_3$ was rapidly heated to 850 K. The spectra did not give characteristic absorption bands for $Ti^{2+}$–Al–Cl but a spectrum almost identical with that of $TiCl_3$ in $Al_2Cl_6$(g). This provides further evidence that $TiCl_2$ disproportionates to $TiCl_3$ and Ti metal, even under these conditions. The only difference was an increased intensity of the shoulder at ~1.4 $\mu m^{-1}$, especially at lower temperatures, indicating that an increased amount of $Ti^{2+}$–Al–Cl(g) is present relative to what was found in the system $TiCl_3$–$Al_2C_6$(g).

It was possible to obtain the spectrum of $Ti^{2+}$–Al–Cl(g) at temperatures up to 725 K by adding Ti metal to a cell containing $AlCl_3$. This gave $Ti^{2+}$ upon reaction with aluminum chloride, but the cell became opaque within a very short time, and no quantitative information was obtained.

It was found, however, that gaseous complexes of $TiCl_2$ were relatively stable in an intermediate temperature range when the condensed phase was a liquid mixture of $TiCl_2$ and $AlCl_3$, but even here some deposition of Ti occurred. Table VIII gives the data for two such experiments in the temperature range 485–608 K. The $Ti^{2+}$–Al–Cl gaseous complex gives a spectrum with two separate peaks, at 0.77 and 1.47 $\mu m^{-1}$ (Figure 11). This spectrum is similar to those previously found for $Ti^{2+}$ in liquid aluminium chloride.[12,26] The net absorption values for the peak at 1.47 $\mu m^{-1}$ are given in Table VIII. The source of divalent titanium was $Ti(AlCl_4)_2$(s) or $TiCl_2$(s). Aluminum metal was added in experiment 15 in an attempt to stabilize $TiCl_2$, but it did not appear to have any significant effect.

It was not possible to perform an independent determination of the molar absorptivity, but the vapor pressure of $Ti^{2+}$–Al–Cl gas complexes has been calculated using the molar absorptivity, $\epsilon_{1.47} = 18.5$ L/(mol cm),[3] for $Ti^{2+}$ in $Al_2Cl_6$(l). It is not expected that this value will introduce any great error, because the spectra showed exactly the same coordination and they were obtained in the same temperature region (compare the

Table VIII. Spectral Data and Vapor Pressures of $Ti^{2+}$–Al–Cl Complexes

| expt no. | specification | $T_{min}$, K | $\overline{T}$, K | $A_{1.47}$ | $P_{Al_2Cl_6}$,[a] atm | $P_{Ti^{2+}-Al-Cl}$, atm |
|---|---|---|---|---|---|---|
| 15 | $l = 10.0$ cm | 485.1 | 491 | $0.009_5$ | 2.192 | 0.002 07 |
| | $V = 54.44$ cm$^3$ | 502.7 | 508 | 0.020 | 2.264 | 0.004 50 |
| | $w_{Ti(AlCl_4)_2} = 0.0729$ g | 518.7 | 524 | 0.035 | 2.328 | 0.008 13 |
| | $w_{AlCl_3} = 0.7922$ g | 531.8 | 537 | 0.050 | 2.379 | 0.011 90 |
| | | 545.8 | 551 | 0.071 | 2.431 | 0.017 34 |
| | $w_{Al} = 0.1533$ g | 558.2 | 564 | 0.096 | 2.476 | 0.024 00 |
| | | 569.1 | 575 | 0.121 | 2.513 | 0.030 84 |
| 16 | $l = 10.0$ cm | 496.1 | 502 | 0.020 | 3.374 | 0.004 45 |
| | $V = 52.85$ cm$^3$ | 513.0 | 519 | 0.038 | 3.481 | 0.008 74 |
| | $w_{TiCl_2} = 0.0115$ g | 530.1 | 536 | 0.063 | 3.583 | 0.014 97 |
| | $w_{AlCl_3} = 1.1842$ g | 545.4 | 551 | 0.089 | 3.671 | 0.021 74 |
| | | 564.7 | 570 | 0.129 | 3.863 | 0.032 59 |
| | | 580.6 | 586 | 0.119 | 3.971 | 0.030 91 |
| | | 592.7 | 598 | 0.114 | 4.050 | 0.030 22 |
| | | 607.6 | 613 | 0.111 | 4.146 | 0.030 16 |

[a] $P_{Al_2Cl_6}$, partial pressure of $Al_2Cl_6$, corrected for dissociation, liquid formation, and complexation.

results for $VCl_2$ in liquid and gaseous $AlCl_3$).[6] The molar absorptivity of $TiCl_2$ in $Al_2Cl_6$(l) showed no significant variation with temperature.

For experiment 16 no further pressure increase of the gas complex was observed above 565 K (Table VIII). At this point no liquid $Ti^{2+}$–Al–Cl was left in the cell, and the gas was in equilibrium with $TiCl_2$(s), which appeared as a black solid. The disappearance of the liquid had a marked effect on the disproportionation of $TiCl_2$. A metal film was soon deposited on the windows inside the cell, making it opaque. Large baseline corrections were necessary, and the three vapor pressure values above 565 K are given with less accuracy than the other data. The complexation reaction with a liquid phase present must be formulated as

$$TiCl_2(TiCl_2\text{–}Al_2Cl_6(l)) + nAl_2Cl_6(g) = TiAl_{2n}Cl_{6n+2}(g) \qquad (XVI)$$

with an equilibrium constant

$$K_{XVI} = \frac{P_{Ti^{2+}-Al-Cl}}{a_{TiCl_2}P_{Al_2Cl_6}{}^{n}} \qquad (16)$$

Although $a_{TiCl_2}$ is dependent on $P_{Al_2Cl_6}$, it is possible to describe the vaporization of $TiCl_2$ by an empirical relation of the form

$$K' = \frac{P_{Ti^{2+}-Al-Cl}}{P_{Al_2Cl_6}{}^{m}} \qquad (17)$$

An average value of $m$ was found to be 0.65. If we reject the experimental values at the temperatures at which $TiCl_2$(s) was present in experiment 16, together with the value for the lowest temperature in experiment 15, a least-squares polynomial fit of the data gave

$$\log K' = -3.014 + \frac{4.418 \times 10^3}{T} - \frac{2.110 \times 10^6}{T^2} \qquad (18)$$

resulting in the empirical relation

$$P_{Ti^{2+}-Al-Cl} = P_{Al_2Cl_6}{}^{0.65} \exp\left(-3.014 + \frac{4.418 \times 10^3}{T} - \frac{2.110 \times 10^6}{T^2}\right) \qquad (19)$$

with a standard deviation of 2.5% within the temperature range studied. Figure 12 gives log $K'$ (=log $(P_{Ti^{2+}-Al-Cl}/P_{Al_2Cl_6}{}^{0.65})$) vs. $1/T$ for experiments 15 and 16.

In order to interpret these results it is necessary to review the properties of mixtures of $AlCl_3$ with high-melting divalent chlorides. Such systems are characterized by a sharply rising liquidus temperature close to the composition $M(AlCl_4)_2$.[27] $AlCl_3$ acts as a chloride-accepting Lewis acid but becomes saturated with respect to chloride when $AlCl_4^-$ is formed stoichiometrically. Consequently, the activity of $AlCl_3$ varies by several orders of magnitude around the composition $M(AlCl_4)_2$, or conversely the melt composition will change only negligibly with changing pressure of $Al_2Cl_6$. The precipitation of $TiCl_2$(s) above 560 K in experiment 16 is an indication that we are close to this composition for experiments 15 and 16.

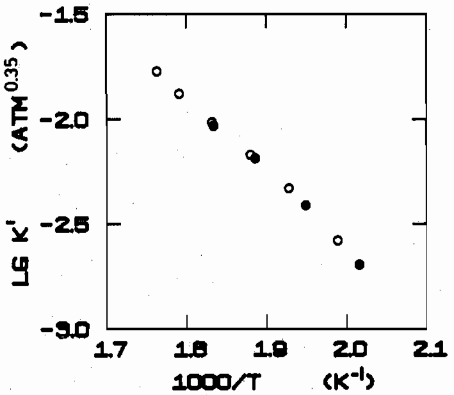

**Figure 12.** Equilibrium constant for the hypothetical reaction $TiCl_2(l) + 0.65Al_2Cl_6(g) = TiAl_{1.3}Cl_{5.9}(g)$: ○, experiment 15; ●, experiment 16.

The present behavior, empirically described by eq 17 with $m$ slightly above 0.5 and precipitation of $MCl_2$(s) at high temperatures, closely parallels the investigation of the gas phase above $EuCl_2$–$AlCl_3$(l), for which a much more thorough study was performed.[28] From that work the only satisfactory conclusion to be drawn is that the melt composition is close to the stoichiometry $Eu(AlCl_4)_2$, and that the composition change is negligible in spite of the fact that the $Al_2Cl_6$ pressure above the melt was varied by a factor of 100. We consider this to be a justification to use the same model for the $TiCl_2$–$AlCl_3$ system. Thus by use of the Gibbs–Duhem equation we obtain similarly

$$a_{TiCl_2} = C\frac{P_{Al_2Cl_6}{}^{\circ}}{P_{Al_2Cl_6}} \qquad (20)$$

where $C$ is an integration constant depending upon the standard state chosen and $P_{Al_2Cl_6}{}^{\circ}$ is the vapor pressure above pure liquid $AlCl_3$.

The quantity $m$ is not a half-integer number and at least two different gaseous species have to be assumed. The pressure of the gaseous complex given by combination of eq 11 and 20 is

$$P_{Ti^{2+}-Al-Cl} = CP_{Al_2Cl_6}{}^{\circ}(K_{XVI}'P_{Al_2Cl_6}{}^{n'-1} + K_{XVI}''P_{Al_2Cl_6}{}^{n''-1}) \qquad (21)$$

Table IX. Spectral Characteristics of Octahedrally Coordinated $Ti^{2+}$

| system | $T$, K | $^3T_{1g}(F) \rightarrow {}^3T_{2g}(F)$ |  | $^3T_{1g}(F) \rightarrow {}^3T_{1g}(P)$, $^3A_{2g}(F)$ |  | ref |
|---|---|---|---|---|---|---|
|  |  | $\bar{\nu}$, $cm^{-1}$ × $10^3$ | ε, L/(mol cm) | $\bar{\nu}$, $cm^{-1}$ × $10^3$ | ε, L/(mol cm) |  |
| $TiCl_2$ in NaCl(s) | 77 | 8.5 | 2.5 | 15.2 | 7.5 | 30 |
| $TiCl_2$ in NaCl(s) | 300 | 8.2 | 2.0 | 14.9 | 10.0 | 30 |
| Monoclinic $Ti(AlCl_4)_2$(s) | 295 | 7.9 |  | 14.8 |  | 12 |
| $TiCl_2$ in $Al_2Cl_6$(l) | 500 | 7.6 | 9.1 | 14.5 | 29.4 | 26 |
| $TiCl_2$ in $Al_2Cl_6$(l) | ~480 | 7.8 | 6.8[a] | 14.7 | 21.0[a] | 12 |
| $TiCl_2$ in $Al_2Cl_6$(l) | 480 | 7.8 | 6.5 | 14.7 | 18.5 | 3 |
| $TiCl_2$ in $Al_2Cl_6$(g) | 558 | 7.7 |  | 14.7 |  | this work |

[a] Corrected value. Private correspondence with Brynestad revealed that their reported molar absorptivity of $Ti^{2+}$ in $Al_2Cl_6$(l) should be multiplied by a factor of 0.4032 ($=M_{Ti}/M_{TiCl_2}$) due to a calculation error.

Because $m$ was found to be 0.65 the most obvious assumptions for the stoichiometries of the gaseous complexes are $TiAl_3Cl_{11}$ and $TiAl_4Cl_{14}$ with the first as the major species. The statistical analysis did not give a full justification for assuming two gaseous species, however, and we chose to take only the major gaseous complex into consideration in spite of a small error involved. Thus,

$$TiCl_2(s) + 1.5Al_2Cl_6(g) = TiAl_3Cl_{11}(g) \quad (XVII)$$

Equation 21 then may be written

$$P_{TiAl_3Cl_{11}} = CP_{Al_2Cl_6}{}^{\circ}K_{XVII}P_{Al_2Cl_6}{}^{0.5} \quad (22)$$

which, through a nonlinear curve fit,[18] yields

$$P_{TiAl_3Cl_{11}} = (P_{Al_2Cl_6})^{1/2} \exp\left(4.550 - \frac{3544}{T}\right) \quad (23)$$

with an overall standard deviation in the pressure of the complex of 4.9%. Lines corresponding to eq 23 have been drawn in Figure 13 in the temperature range where the liquid mixture is present (see previous discussion). The quantity $C$ was assumed to be constant and ln $P_{Al_2Cl_6}{}^{\circ}$ and ln $K$ to be linear functions of $1/T$ within the limited temperature range studied.

From JANAF[1] it is found that

$$P_{Al_2Cl_6}{}^{\circ} = \exp\left(3.744 - \frac{1532}{T}\right) \quad (24)$$

around 600 K. The integration constant $C$ was found to be 0.32 from experiment 16, setting $a_{TiCl_2} = 1$ at $T = 560$ K. The thermodynamic parameters for eq XVII can then be estimated. The combination of eq 22–24 yields

$$\log K_{XVII} = 1.301 - \frac{2012}{T} \quad (25)$$

giving at 600 K $\Delta H_{XVII}{}^{\circ} = 38.5$ kJ and $\Delta S_{XVII}{}^{\circ} = 24.9$ J/K.

Care must be exercised in using these values because of the uncertainties involved and the approximations made. Nevertheless the values obtained are acceptable in view of previous studies of divalent 3d metal ions; see for instance ref 29.

Compared to $TiCl_3$ in an aluminum chloride atmosphere, the increased vapor pressure of $TiCl_2$ in aluminum chloride is of a totally different order of magnitude. The volatility of $TiCl_2$(s) in 1 atm of $Al_2Cl_6$ is increased by a factor of $10^{12.3}$ relative to $P_{TiCl_2}$ above $TiCl_2$(s) at 600 K.[1]

**(b) Coordination.** The spectra of the gaseous $Ti^{2+}$–Al–Cl complex are strikingly similar to the spectra of $TiCl_2$ in $Al_2Cl_6$(l) obtained by Øye and Gruen,[26] which they attributed to octahedrally coordinated $Ti^{2+}$. Their interpretation later was confirmed by the work of Brynestad et al.[12] on $Ti(AlCl_4)_2$ and of Smith[30] on isomorphic substitution of $TiCl_2$ in NaCl(s).

It is suggested that $Ti^{2+}$ is octahedrally coordinated in the gaseous complex, the two bands at 1.47 and 0.77 $\mu m^{-1}$ being the electronic transitions $^3T_{1g}(F) \rightarrow {}^3T_{1g}(P)$, $^3A_{2g}(F)$ and $^3T_{1g}(F) \rightarrow {}^3T_{2g}(F)$, respectively. At high temperatures the absorption band at 1.47 $\mu m^{-1}$ was shifted somewhat toward lower energies accompanied by a small increase in half-width.

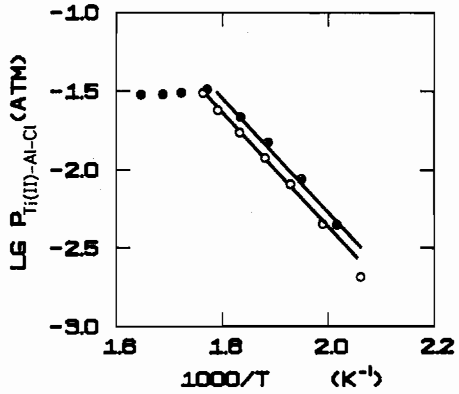

**Figure 13.** Experimental vapor pressure of $Ti^{2+}$–Al–Cl(g) complexes in equilibrium with $TiCl_2$(s), $TiAl_2Cl_8$(l), and $Al_2Cl_6$(g): ○, experiment 15; ●, experiment 16; —, eq 23.

Table IX lists the spectral characteristics of coordinated $TiCl_2$ in the solid, liquid, and gaseous states.

## Concluding Remarks

**Stabilities of Titanium Chlorides in the Presence of $Al_2Cl_6$(g).** No detectable gaseous complex between $Al_2Cl_6$(g) and $TiCl_4$(g) was observed. Hence, $Al_2Cl_6$(g) does not affect the vapor-phase stability or red–ox properties of $TiCl_4$(g).

Figure 14 illustrates the vaporization characteristics of di- and trivalent titanium chloride in an $Al_2Cl_6$ atmosphere. The upper curves show the apparent vapor pressures of di- and trivalent titanium chlorides as gaseous complexes above the stable, condensed phase in an $Al_2Cl_6$ atmosphere at a total pressure of 1 atm. For this pressure $TiAl_2Cl_8$(l) is the stable divalent phase up to about 200 °C, while $TiCl_2$(s) is stable above this temperature. The stable trivalent condensed phase is $TiCl_3$(g) over the entire experimental range studied. Higher vapor pressure of $Al_2Cl_6$ will extend the stability region of $TiAl_2C_8$(l) to higher temperatures.

For comparison the vapor pressures of $TiCl_2$ and $TiCl_3$ above their pure solid chlorides in an inert atmosphere are also given. Addition of $Al_2Cl_6$(g) results in a substantial increase of the apparent vapor pressure of the di- and trivalent chlorides. Although the vapor pressure of pure $TiCl_2$ is lower by several orders of magnitude than to that of pure $TiCl_3$, $Al_2Cl_6$(g) is seen to raise the apparent vapor pressure of the divalent chloride far more than that of the trivalent. Thus, the apparent vapor pressure of divalent chloride is almost equal to that of the trivalent chloride at 600 K. Hence, it may be concluded that $Al_2Cl_6$(g) increases the stability of divalent titanium chloride in the vapor phase far more than it does for the trivalent compound.

The gas complexation of trivalent titanium, however, results in a reduced stability of divalent titanium toward dispro-

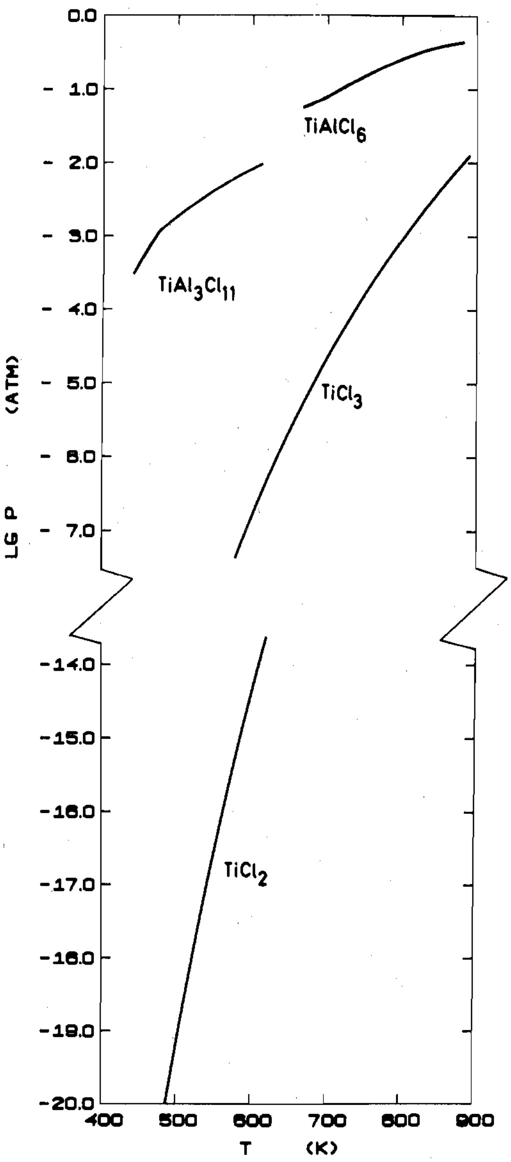

**Figure 14.** Partial pressure of Ti–Al–Cl complexes above $TiAl_2Cl_8(l)$, $TiCl_2(s)$, and $TiCl_3(s)$ in $Al_2Cl_6$ atmosphere at a total pressure of 1 atm together with the sublimation pressures of $TiCl_2(s)$ and $TiCl_3(s)$.

portionation to Ti(s). This is readily seen by comparing the disproportionation reaction with aluminium chloride, thus

$$3\mathrm{TiCl_2(s)} + \mathrm{Al_2Cl_6(g)} = \mathrm{Ti(s)} + 2\mathrm{TiAlCl_6(g)} \qquad \text{(XVIII)}$$

having log $K_{600} = -10.6$. The disproportionation without aluminum chloride (reaction II) has log $K_{600} = -20.1$.

Both equilibrium constants increase with rising temperature. The increasing background seen on Figure 11 is due to deposition of Ti(s) from reaction XVIII.

A similar destabilization of $TiCl_3(s)$ to $TiCl_2(s)$ and $TiCl_4(g)$ upon addition of $Al_2Cl_6$ does not take place because $TiCl_4(g)$ does not form complexes with $Al_2Cl_6(g)$.

**Chemical Vapor Deposition of Metallic Titanium.** As mentioned earlier, considerable difficulties were encountered in the study of gaseous complexes of divalent titanium due to the formation of metallic titanium. These difficulties and the ease with which titanium was formed point to a possibly interesting technical application of the Ti–Al–Cl system for vapor deposition or for purification of metallic titanium at moderate temperatures.

Figure 1 illustrates a typical observation. The initial $TiCl_2(s)$ remains in the middle of the cell where the temperature is lower. Ti(s) is then deposited on the hottest part of the cell, i.e., the windows, while $TiCl_3(s)$ is deposited in the middle of the cell. No evidence has been found for Ti being transported as metallic or as subvalent species with an oxidation number between 0 and 2.

The observation may be understood from the gas complex reactions encountered and may be formulated as follows. Gas complexation of $TiCl_2$ above the cold part occurs according to reaction XVII with log $K_{XVII} = -2.1$ at 600 K. Disproportionation and deposition on hot parts proceed according to the reaction

$$3\mathrm{TiAl_3Cl_{11}(g)} = \mathrm{Ti(s)} + 3.5\mathrm{Al_2Cl_6(g)} + 2\mathrm{TiAlCl_6(g)} \qquad \text{(XIX)}$$

(At 600 K $\Delta H_{XIX}° = 142$ kJ, $\Delta S_{XIX}° = 153$ J/K, and log $K_{XIX} = -4.4$.) Chemical transport of trivalent titanium from the hot to the cold parts occurs through reversal of reaction XII; thus

$$\mathrm{TiAlCl_6(g)} = \mathrm{TiCl_3(s)} + {}^1/_2\mathrm{Al_2Cl_6(g)} \qquad \text{(XX)}$$

(At 600 K $\Delta H_{XX}° = -77$ kJ, $\Delta S_{XX}° = -89$ J/K, and log $K_{XX} = 2.1$.)

Due to the high stability of $TiAl_3Cl_{11}(g)$, reaction XIX has the positive $\Delta H°$ that is needed for a hot-spot disproportionation and deposition of Ti(s), and trivalent titanium will be back-transported through the other gaseous complex, $TiAlCl_6$ (reaction XX).

In the absence of $Al_2Cl_6$ such a mechanism does not give any appreciable deposition of Ti because of the small equilibrium constants and low vapor pressures.

The transport of Ti(s), described above, is probably responsible for the failure to stabilize the divalent state by addition of Ti or Al metal to the cell but does, however, provide an important reaction for producing pure metallic Ti either from impure Ti or through reduction of titanium chlorides with aluminium. Work is in progress to characterize the vapor deposits of metallic titanium.

**Acknowledgment.** Discussions with Mr. J. Brynestad, Dr. H. Kvande, Dr. T. Rosenqvist, and Dr. J. Toguri at various stages of this work are highly appreciated. Financial support from "Norges almenvitenskapelige forskningsråd" and later from Alcoa Foundation and "Norges teknisk-naturvitenskapelige forskningsråd" is gratefully acknowledged.

**Registry No.** $TiCl_2$, 10049-06-6; $TiCl_3$, 7705-07-9; $TiCl_4$, 7550-45-0; $Al_2Cl_6$, 13845-12-0; $Ti_2Cl_6$, 31135-25-8; $TiAlCl_6$, 58260-40-5; $TiAl_3Cl_{11}$, 67113-71-7.

## References and Notes

(1) "JANAF Thermochemical Tables", *Natl. Stand. Ref. Data Ser., Natl. Bur. Stand.*, **No. 37** (1971).
(2) L. D. Polyachenok, G. I. Novikov, and O. G. Polyachenok, *Obshch. Prikl. Khim.*, 45 (1972).
(3) M. Sørlie and H. A. Øye, to be submitted for publication.
(4) H. A. Øye and D. M. Gruen, *J. Am. Chem. Soc.*, **91**, 2229 (1969).
(5) E. W. Dewing, *Met. Trans.*, **1**, 2169 (1970).
(6) A. Anundskås and H. A. Øye, *J. Inorg. Nucl. Chem.*, **37**, 1609 (1975).
(7) K. Grjotheim, C. Krohn, and H. A. Øye, *Aluminium (Duesseldorf)*, **51**, 697 (1975).
(8) H. H. Glaeser, U.S. Patents 3926614 (1975), 3977862, 3977864 (1976).
(9) M. Ogushi, *Chem. Econ. Eng. Rev.*, **8**, 49 (1976).
(10) O. Borgen, T. Bruvoll, and H. Petersen, "A Data Collection and Recording System for the CARY 17H Spectrophotometer", Technical Report 70, Division of Physical Chemistry, University of Trondheim, NTH, 1976.
(11) G. Brauer, "Handbuch der präparativen Anorganischen Chemie", Ferdinand Emke Verlag, Stuttgart, 1960.
(12) J. Brynestad, S. v. Winbush, H. L. Yakel, and G. P. Smith, *Inorg. Nucl. Chem. Lett.*, **6**, 889 (1970).
(13) D. S. Alderdice, *J. Mol. Spectrosc.*, **15**, 509 (1965).
(14) L. Di Sipio, G. De Michelis, E. Tondello, and L. Oleari, *Gaz. Chim. Ital.*, **96**, 1785 (1966).
(15) C. Dijkgraaf and J. P. G. Rousseau, *Spectrochim. Acta, Part A*, **24**, 1213 (1968).
(16) A. A. Iverson and B. R. Russel, *Spectrochim. Acta, Part A*, **29**, 715 (1973).
(17) E. Sibbing and H. Schäfer, *Z. Anorg. Allg. Chem.*, **410**, 67 (1974).
(18) T. Hertzberg, "MODTLP-A General Computer Program for Fitting of Non-Linear Models to Experimental Data", Chemical Engineering Laboratory, University of Trondheim, 1970 (in Norwegian).

(19) P. Gross, *Can. Metall. Q.*, **12**, 359 (1973).
(20) D. Altman, M. Farber, and D. M. Mason, *J. Chem. Phys.*, **25**, 531 (1956).
(21) B. S. Sanderson and G. E. MacWood, *J. Phys. Chem.*, **60**, 314 (1956).
(22) B. S. Sanderson and G. E. MacWood, *J. Phys. Chem.*, **60**, 316 (1956).
(23) J. W. Hastie, "High Temperature Vapors", Academic Press, New York, N.Y., 1975, p 21.
(24) C. Dijkgraaf and J. P. G. Rousseau, *Spectrochim. Acta, Part A*, **23**, 1267 (1967).
(25) D. M. Gruen and R. L. McBeth, *Pure Appl. Chem.*, **6**, 23 (1964).
(26) H. A. Øye and D. M. Gruen, *Inorg. Chem.*, **3**, 836 (1964).
(27) E. M. Levin, C. R. Robbins, and H. F. McMurdie: "Phase Diagrams for Ceramists", The American Ceramic Society, Columbus, Ohio, 1964 (Supplement 1969, 1975).
(28) M. Sørlie and H. A. Øye, *J. Inorg. Nucl. Chem.*, **40**, 493 (1978).
(29) H. Schäfer, *Angew. Chem.*, **88**, 775 (1976).
(30) W. E. Smith, *J. Chem. Soc., Chem. Commun.*, 1121 (1972).

---

Contribution from the Department of Chemistry,
Kansas State University, Manhattan, Kansas 66506

# Direct Synthesis of Fluorinated Peroxides. 8. Synthesis and Properties of $(CF_3)_3COOF$ and Evidence for the Trioxide $(CF_3)_3COOOC(CF_3)_3$

SHIN-LIANG YU and DARRYL D. DESMARTEAU*[1]

*Received December 15, 1977*

The preparation of $(CF_3)_3COOF$ has been achieved by the low-temperature reaction of fluorine with the novel peroxo anion $(CF_3)_3COO^-$. The latter is generated in situ by nucleophilic attack of fluoride on $(CF_3)_3COOSO_2F$. The compound has been characterized by $^{19}F$ NMR, infrared, and Raman spectroscopy and by its thermal decomposition and addition to chlorotrifluoroethylene. Reaction of $(CF_3)_3COOF$ with $KOC(CF_3)_3$ forms the unstable trioxide $(CF_3)_3COOOC(CF_3)_3$.

## Introduction

Several members of the new class of fluorinated peroxides containing the perfluoro-*tert*-butyl group have recently been described.[2] These new compounds were obtained from $(CF_3)_3COOC(O)F$ which was obtained by a novel nucleophilic displacement reaction with $(CF_3)_3COOSO_2F$ in the presence of $COF_2$ and KF (eq 1). This reaction probably involves the formation of the unstable anion $(CF_3)_3COO^-$. By employing CsF instead of KF, it has now been possible to generate this anion at low temperature and to carry out its controlled oxidation by fluorine, forming $(CF_3)_3COOF$ in excellent yield. This new method of preparation may have general applicability.

$$(CF_3)_3COOSO_2F + COF_2 \xrightarrow{KF} (CF_3)_3COOC(O)F + SO_2F_2 \tag{1}$$

In previous work by us on the synthesis of fluorinated peroxygen compounds containing the trifluoromethyl and pentafluorosulfur groups, the hydroperoxides $CF_3OOH^{4-7}$ and $SF_5OOH^{8-10}$ have been key reagents. The corresponding perfluoro-*tert*-butyl hydroperoxide, $(CF_3)_3COOH$, is much more difficult to prepare and is thus of less use in the direct synthesis of $(CF_3)_3COO$ derivatives. The easy synthesis of $(CF_3)_3COOF$ described here makes it the most accessible reagent for this purpose. This paper presents details for its preparation and describes some of its physical and chemical properties.

## Experimental Section

**General Procedures.** Volatile compounds were handled in a glass and stainless steel vacuum system equipped with glass–Teflon or stainless steel valves. Pressures were measured with a Wallace and Tiernan differential pressure gauge, series 1500. All reactions were carried out in 75-mL 304 stainless steel reactors or glass bulbs fitted with glass–Teflon valves. Separation of volatile products was by trap-to-trap distillation and GLC using columns packed with 40% halocarbon 11-21 polymer oil on Chromosorb P.

Infrared spectra were recorded on Perkin-Elmer Model 180 or 337 spectrophotometers using a 10-cm gas cell fitted with AgCl windows. Raman spectra were recorded at low temperatures using a Spex 14018 monochromater with photon counting detection. A low-temperature cell similar to that described by Brown et al.[11] was employed. Excitation was by the 514.5-nm line of an argon laser or by a tunable CW dye laser output in the 610-nm region. NMR spectra were recorded with a Varian XL-100-15 spectrometer in CW or pulsed FT modes using ~15 mol % solutions in $CFCl_3$.

**Reagents.** Fluorine, CsF, KH, $CF_2CFCl$, and $(CF_3)_3COH$ were obtained from commercial sources. $(CF_3)_3COOSO_2F$ was prepared by the reaction of $S_2O_6F_2$ with $KOC(CF_3)_3$.[12] Peroxydisulfuryl difluoride was prepared by heating stoichiometric amounts of $2SO_3$ and $F_2$ at 160 °C in a 150-mL bomb, loosely packed with Ag-coated copper gauze. The vessel was heated with 5 atm of $F_2$ at 200 °C before adding $SO_3$ and $F_2$. On a 100-mmol scale, yields were quite high with small amounts of unreacted $SO_3$, $O_2$, and $SO_2F_2$. Treatment with concentrated $H_2SO_4$ and collection at –78 °C provided pure $S_2O_6F_2$. Preparation of $KOC(CF_3)_3$ was by reaction of the alcohol with KH in ether at 0 °C, followed by filtration and evaporation of the diethyl ether solvent.[13] Fluorine was passed through a NaF scrubber before use. CsF was dried in a metal reactor at 80 °C under dynamic vacuum for 17 h and then treated with ~2 atm of $F_2$ for several hours. The metal reactor contained several nickel balls up to $^1/_4$ in. During treatment with $F_2$, the vessel was agitated violently on a paint shaker for ~5 min.

**Preparation of $(CF_3)_3COOF$.** The reaction of $(CF_3)_3COOSO_2F$ with fluorine in the presence of CsF was carried out under a variety of conditions. The following procedure normally produced the highest yields. Into a 75-mL metal reactor containing 15 g of activated CsF, 2.7 mmol of $(CF_3)_3COOSO_2F$ and 6.0 mmol of $F_2$ were added at –196 °C. The reactor was placed in a large Dewar filled with an ethanol–water slush at –55 °C. After 24 h, the bath temperature was –35 °C. The contents were collected at –196 °C and then fractionated through traps at –65, –95, and –196 °C. The –65 °C trap contained a small amount of $(CF_3)_3COOC(CF_3)_3$[14] identified by IR and NMR spectroscopy and molecular weight. The –95 °C trap contained nearly pure $(CF_3)_3COOF$ with small amounts of $(CF_3)_3COF$.[15] The –196 °C trap contained $SO_2F_2$ with small amounts of $CF_4$, $C_2F_6$, and other products. If there is unreacted $(CF_3)_3COOSO_2F$ (depending on the activity of the CsF), the –65 and –95 °C traps will both contain the fluorosulfate. It can only be effectively removed from $(CF_3)_3COOF$ by GLC with some loss of $(CF_3)_3COOF$ from decomposition. The best yields of $(CF_3)_3COOF$ were ~80%. $(CF_3)_3COOF$: mp –17 to –16 °C: mol wt found 270.4, calcd 270.0. IR: 1310–1260 (vs), 1069 (s), 1009 (s), 987 (s), 760 (w), 741 (s), 537 (w), 499 (w) $cm^{-1}$. Raman (liquid, –15 °C) [$cm^{-1}$, relative intensity, polarization]: 1284, br; 1003, 1.2, p; 989, sh; 902, 1.0, p; 768, 10, p; 741, 1.2, p; 724, 0.7, dp; 633, 0.2, dp; 570, 0.4, dp; 540, 0.7, dp; 503, sh; 489, 1.2, p; 489, 1.2, p; 484, sh; 441, 0.1, p; 359, 1.6, p; 331, sh; 314, 4.1, p; 304, sh; 297, sh; 233, 1.2, p; 204, 0.2, dp; 184, 0.1, p; 174, 0.1, p; 160, 0.5, dp; 136,

0020-1669/78/1317-2484$01.00/0